Inorganic Chemistry Research

Article

Synthesis of Cr_2O_3 Nanoparticles Encapsulating Phosphotungstic Acid as an Efficient Photocatalyst to Degrade Methadone

Farshid Kazemi[a], Hassan Ali Zamani[a,*], Mohammad Reza Abedi[b] and Mahmoud Ebrahimi[a]

[a]*Department of Applied Chemistry, Mashhad Branch, Islamic Azad University, Mashhad, Iran*
[b]*Department of Applied Chemistry, Quchan Branch, Islamic Azad University, Quchan, Iran*

Received: December 1, 2021; Accepted: January 19, 2022
Cite This: *Inorg. Chem. Res.* **2022**, *6*, 31-38. DOI: 10.22036/icr.2022.317862.1121

Abstract: Methadone is a synthetic drug utilized to manage chronic pain and treat opioid maintenance. The drug enters water bodies as a contaminant due to its widespread use in various communities, which is usually not removed by wastewater treatment plants. Therefore, a photodegradation procedure was developed to degrade and remove methadone in water samples. A hydrothermal strategy was applied to prepare three photocatalysts based on Cr_2O_3 nanoparticles, a polyoxometalate (phosphotungstic acid), and a hybrid material (Cr_2O_3 nanoparticles encapsulating phosphotungstic acid). The effective factors, such as methadone concentration, pH, photocatalyst amount, and H_2O_2 concentration, in the photodegradation method for each catalyst were optimized by an experimental design using a central composite design. Under the optimum conditions, the kinetic model and maximum photodegradation efficiency of the process for each catalyst were studied to compare their ability for methadone degradation. The maximum photodegradation efficiencies for methadone degradation using phosphotungstic acid and Cr_2O_3 nanoparticles were 82.00 and 77.18% for 120 min. In comparison, the maximum photodegradation efficiency in the presence of Cr_2O_3 nanoparticles encapsulating phosphotungstic acid was 90.11% for 100 min. The results indicated the new hybrid material prepared from encapsulating phosphotungstic acid with Cr_2O_3 nanoparticles, leading to a proper increase in the methadone degradation and reducing the degradation time significantly.

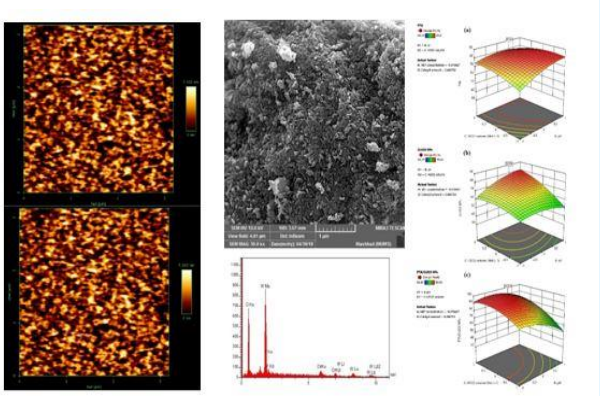

Keywords: Methadone; Photodegradation technique; Phosphotungstic acid; Cr_2O_3 nanoparticles; Hydrothermal synthesis; Hybrid material

1. INTRODUCTION

Methadone (MET) is a synthetic drug widely used to manage chronic pain and treat opioid maintenance in people with opioid dependence.[1, 2] Due to their widespread use of opioid drugs, a lot amount of these drugs have entered the environment, leading to biological contamination of water sources with a concentration range of ng L^{-1} to µg L^{-1} in wastewater. Unfortunately, wastewater treatment plants (WWTPs) are generally unable to remove these drugs from drinking water.[3] Therefore, it is necessary to provide proper methods for removing opioid drugs, especially MET, to reduce their concentration in water bodies and their adverse effects on humans and animals. The photodegradation technique is an excellent way to remove various contaminants, especially organic compounds, from water sources.[4-7] The method can be performed under mild conditions with a low cost, energy, and reagent consumption.[8, 9] In the procedure, The energy of the ultraviolet or visible photons exposed to a wastewater sample in the presence of a suitable catalyst is converted directly into chemical energy to form electron-hole pairs, which leads to the formation of free radicals to degrade pollutants.[5] Obviously, photocatalyst play a critical role in the procedure to achieve high degradation efficiency toward pollutants.[10, 11]

Nanoparticles and nanocomposites are a wide range of compounds with suitable properties as heterogeneous catalysts, such as appropriate flexibility, simple preparation, easy tenability, high porosity and surface area, and tuneable pore size.[12-14] They were synthesized using various procedures, including solvothermal, electrochemical, mechanochemical, hydrothermal, and sonochemical methods.[15-17] The hydrothermal strategy has performed a reaction between a metal salt with other materials and an organic solvent in an autoclave. The procedure was usually followed by calcinating under a proper temperature. The mixture was heated and

calcinated at appropriate temperatures to control the morphology of nanoparticles and nanocomposites and lead to a high yield.[18-21] Therefore, the preparation or selection of nanoparticles with proper stability and suitable activity is vital for their applications as catalysts in water media.

Polyoxometalates (POMs) are a group of transition metal oxide clusters composed of the highest oxidation transition metal cations, such as tungsten or molybdenum ions.[22] In the structure of POMs, the chemical bonds were formed between the transition metal cations and the oxo ligands to prepare POMs leading to unique properties such as simple preparation, high stability, low cost, easy tenability, low toxicity, high surface area with a high ability to absorb ultraviolet light.[23-26] The photocatalytic activity of POMs is usually due to easily excitation of anions of POMs under UV light, leading to a degradation of pollutions.[27] Changes in the type of elements and lattice structure in POMs are very effective in the ability of these compounds to absorb photons and form electron-hole pairs.[22] Also, the preparation of various hybrid materials of POMs with Nanoparticles has received much attention, which improves the photocatalytic activity and stability of the prepared hybrid compounds.[28-30]

In the study, a photodegradation procedure was developed to degrade MET in water media under ultraviolet waves. For this purpose, three photocatalysts, including Cr_2O_3 nanoparticles, a POM (Phosphotungstic acid), and Cr_2O_3 nanoparticles encapsulating phosphotungstic acid, were synthesized using a hydrothermal technique. The effective factors in the photodegradation method were investigated and optimized using central composite design to reduce runs, reagents and time consumption and to evaluate the effects of factors interaction. The kinetic of the photodegradation process was studied in the presence of three catalysts to compare their ability for MET degradation.

2. EXPERIMENTL

Material and instrument

Methadone (MET) was obtained from Amin Pharma Co. (Isfahan, Iran). Other materials such as Chromium(VI) oxide, phosphotungstic acid hydrate (PTA), and ethanol were purchased from Merck (Germany).

The MET concentration in water samples was determined using a UV-Vis spectrophotometer (Varian Cary Bio 50 model) at 292 nm in 0.1 M HCl**.** The morphology of PTA, Cr_2O_3 nanoparticles, and PTA/Cr_2O_3 nanoparticles as photocatalyst were evaluated using the Fourier transform infrared spectrophotometer (FTIR, Tensor model, Bruker, Germany), the field-emission scanning electron microscopy (FE-SEM; Mira 3 Tescan; Czech Republic), and X-ray diffraction (XRD, Philips Xpert-pw3040/60, Netherlands). A UVC lamp (36 W, FPL, 4 pins, Mazda, Japan) was used to investigate the photocatalytic activity of PTA, Cr_2O_3 nanoparticles, and PTA/Cr_2O_3 nanoparticles for the MET degradation. The pH of samples was determined or adjusted by a Metrohm pH meter (model 780, Switzerland).

Synthesis of PTA/Cr_2O_3 nanoparticles

A hydrothermal procedure was used to prepare PTA/Cr_2O_3 nanoparticles. Typically, 5.0 g of CrO_3 and 4.8 g PTA and 2.52 mL of ethanol were poured into 60.0 mL of distilled water, followed by sonicating for 30 min at room temperature. The mixture was transferred into an autoclave and heated in an oven for 2 h at 190 °C. The product was separated, washed using distilled water two times, and finally dried at 80 °C for 10 h in an oven. The product was then calcinated for 1h at 400 °C to prepare PTA/Cr_2O_3 nanoparticles. Also, Cr_2O_3 nanoparticles were also prepared according to the above procedure without adding TPA to compare their photocatalytic activities.[31]

Degradation procedure

A proper amount of PTA/Cr_2O_3 nanoparticles as a photocatalyst and hydrogen peroxide (2.0 mL) were poured into a MET solution (15.0 mL), followed by adjusting its pH to 4.7 using an aqueous solution of NaOH or HCl (0.1 mol L^{-1}). The resulted mixture was stirred by a magnetic stirrer at 200 rpm for 30 min before exposing it with a UVC lamp to achieve an equilibrium. A UVC lamp (36 W, FPL, 4 pins, Mazda, Japan) was used to expose the mixture. The lamp was placed at a distance of 10 cm above the mixture, followed by stirring at 200 rpm for different times. The temperature of the homemade system was controlled using a suitable fan the temperature in the system from increasing. PTA/Cr_2O_3 nanoparticles were thoroughly centrifuged at 5000 rpm for 6 min to separate the catalyst. The methadone concentration in the obtained solution was determined at 292 nm in 0.1 M HCl by a UV-Vis spectrophotometer. The following equation was utilized to calculate the methadone photodegradation efficiency (PE%):

$$PE\% = \frac{C_i - C_f}{C_i} \times 100 \quad (1)$$

In the equation, C_f, and C_i are the MET concentration in the final solution and initial solution, respectively. A schematic of the MET degradation process is shown in Figure 1.

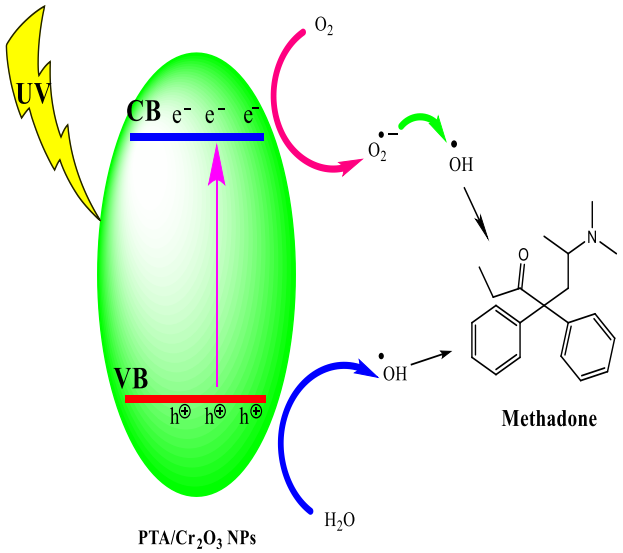

Figure 1. Schematic of the MET degradation process.

3. RESULTS AND DISCUSSION

Characterization of PTA/Cr_2O_3 nanoparticles

FTIR spectrum of PTA/Cr_2O_3 nanoparticles is shown in Figure 2. The adsorption peak at 3410 cm^{-1} corresponded to stretching of O-H groups for nondissociated water absorbed in PTA/Cr_2O_3 nanoparticles, respectively. Besides, the bending vibration of nondissociated water in PTA/Cr_2O_3 nanoparticles is at a wavenumber of 1644 cm^{-1}. The adsorption peak at 529 cm^{-1} is related to O-Cr-O groups on Cr_2O_3 nanoparticles. The presence of these peaks confirmes the successful synthesis of Cr_2O_3 nanoparticles in the catalyst structure. The adsorption peaks at 1087, 841, and 773 cm^{-1} are related to the vibration of P=O, W-O-W, and W-O-O functional groups in PTA.

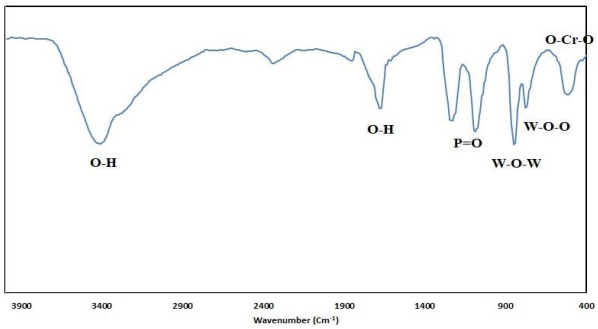

Figure 2. FTIR spectrum of PTA/Cr_2O_3NPs.

SEM images of PTA/Cr_2O_3 nanoparticles and Cr_2O_3 nanoparticles are presented in Figure 3. The Cr_2O_3 nanoparticles have a spherical shape with a size of 20-70 nanometers, which are aggregated mainly. There are many pores with different sizes in the structure of these nanoparticles (Figure 3a). Figure 3b showed that the catalyst surface was formed from various nanoparticles with an oval and spherical shape. Spherical nanoparticles are most likely Cr_2O_3 nanoparticles dispersed in PTA oval nanoparticles. The nanoparticles were aggregated and formed pores of multiple sizes irregularly on the catalyst surface. The oval nanoparticles on the catalyst surface have a length in the range of 80-150 nm and a width between 40-80 nm approximately.

EDX pattern of PTA/Cr_2O_3 nanoparticles is shown in Figure 3c, indicating that the prepared catalyst was formed from different elements such as carbon, oxygen, phosphor, tungsten and chromium. Besides, Three elements (carbon, oxygen, and tungsten) have the highest percentage in the catalyst.

AFM patterns of PTA/Cr_2O_3 nanoparticles is presented in Figure 4a and b. These patterns were applied to evaluate the prepared catalyst surface. A scanning area of 3 µm×3 µm was used to obtain these images. Based on the results, the root mean square value of PTA/Cr_2O_3 nanoparticles as a catalyst is low and equal to 1.443, indicating that the

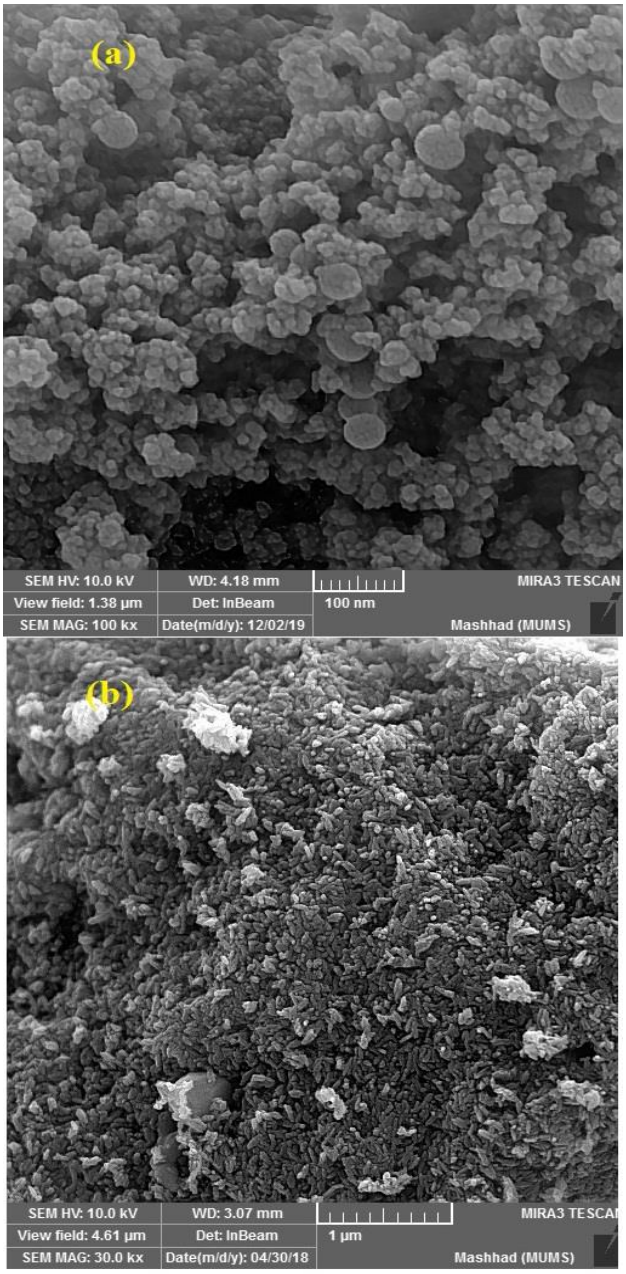

Figure 3. EFSEM Cr_2O_3NPs (a) and PTA/Cr_2O_3NPs (b), and EDX pattern of PTA/Cr_2O_3NPs.

catalyst has a low superficial roughness and smooth surface. However, a suitable photocatalytic activity of PTA/Cr_2O_3 nanoparticles to degrade MET may be obtained due to a non-uniform catalyst surface to absorb ultraviolet waves.

XRD pattern of PTA/Cr_2O_3 nanoparticles is shown in Figure 4c. The Cr_2O_3 nanoparticles in the catalyst structure have a hexagonal structure with a JCPDS Card 38-1479. The planes of diffraction peaks for the Cr_2O_3 nanoparticles are presented in Figure 4C. The presence of PTA in the catalyst structure was confirmed based on a JCPDS Card 75-2125.

Photodegradation optimization

Several factors such as the MET concentration, pH, hydrogen peroxide volume, and catalyst amount were selected as effective parameters for the MET degradation using PTA, Cr_2O_3 nanoparticles, or PTA/Cr_2O_3 nanoparticles as a photocatalyst. For this purpose, a design based on the central composite design was created to optimize these factors. The design consisted of 30 experiments performed in a random order to eliminate the effect of unknown and uncontrollable factors. Each run was carried out under the same conditions three times, and the average photodegradation efficiencies of methadone were calculated. The design and the obtained PEs for three catalysts are shown in Table 1. The obtained PE% for each catalyst were evaluated using analysis of variance (ANOVA) based on the p-value of each factor or interaction at a confidence interval of 95%. The results are summarized in Table 2. The presented models for investigating the effects of all factors and their interactions on the MET degradation using PTA, Cr_2O_3 nanoparticles, or Cr_2O_3 nanoparticles as a photocatalyst were significant because the p-values of the models were lower than 0.05 (a significant parameter); In contrast, the p-values of lack of fits were higher than 0.05 (a non-significant parameter). All selected factors showed meaningful effects on the MET degradation due to the p-values lower than 0.05 for three catalysts. Also, three interactions, including the interactions between MET concentration and pH (AB), pH and H_2O_2 concentration (BC), and H_2O_2 concentration and catalyst amount (CD), have significant effects on the MET degradation for all catalysts. In contrast, the interaction between MET concentration and catalyst amount (AD) and interaction between pH and catalyst amount (BD) are nonmeaningful interactions for the MET degradation for all catalysts. Finally, the interaction between MET concentration and H_2O_2 concentration (AC) has a significant effect on the MET degradation using PTA as a photocatalyst and a nonsignificant effect using Cr_2O_3 nanoparticles or PTA/Cr_2O_3 nanoparticles as a photocatalyst.

A quadratic equation was selected to describe the relationship between the obtained PEs with factors and

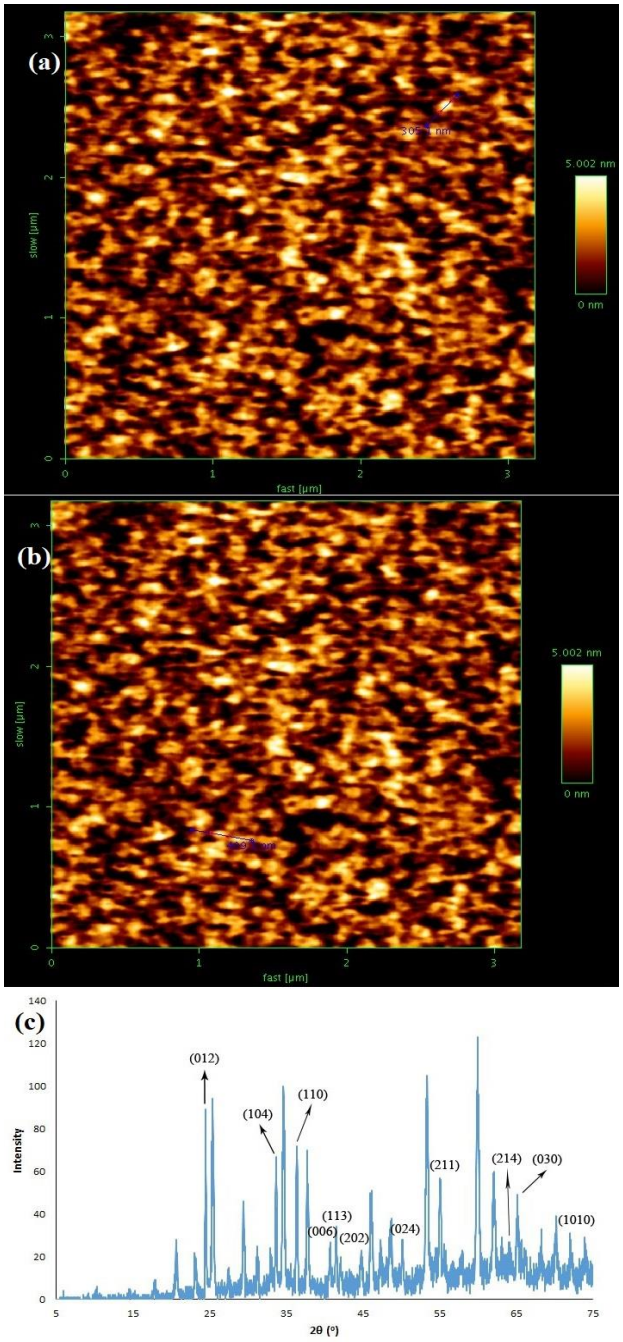

Figure 4. EFM (a and b) and XRD (c) pattern of PTA/Cr_2O_3NPs.

interactions. The obtained equations for the MET degradation using PTA, Cr_2O_3 nanoparticles, or PTA/Cr_2O_3 nanoparticles as a photocatalyst are presented as follows;

PE% (PTA) = 77.2733 - 6.35833 * A + 6.44167 * B + 2.825 * C + 6.275 * D + 3.6325 * AB - 1.3125 * AC - 0.3125 * AD - 4.1825 * BC + 0.4375 * BD - 3.2075 * CD - 3.83125 * A^2 - 4.08125 * B^2 - 3.58125 * C^2 - 4.20625 * D^2 (2)

Table 1. Central composite design for the optimization of MET degradation

Factor	Name	Units	Minimum	Center	Maximum
A	MET concentration	mg L^{-1}	100	200	300
B	pH	-	3.0	5.5	8.0
C	H_2O_2 concentration	mol L^{-1}	0.3	0.4	0.6
D	Catalyst amount	mg	100	150	200

Std	Run	A	B	C	D	PTA	Cr_2O_3 NPs	PTA/Cr_2O_3NPs
23	1	0	0	0	-2	48.69	33.69	41.69
28	2	0	0	0	0	81.4	70.36	89.23
9	3	-1	-1	-1	1	66.41	50.81	71.31
27	4	0	0	0	0	61.49	67.46	90.49
15	5	-1	1	1	1	72.93	79.41	72.91
29	6	0	0	0	0	76.51	72.16	91.09
20	7	0	2	0	0	76.29	63.29	45.69
24	8	0	0	0	2	74.29	71.29	85.29
16	9	1	1	1	1	67.77	77.85	93.35
13	10	-1	-1	1	1	77.01	61.01	87.11
4	11	1	1	-1	-1	57.81	47.41	41.31
25	12	0	0	0	0	79.13	68.83	87.17
7	13	-1	1	1	-1	67.17	49.57	47.07
22	14	0	0	2	0	68.89	65.89	80.49
11	15	-1	1	-1	1	82.81	40.73	36.63
8	16	1	1	1	-1	62.01	64.01	63.51
17	17	-2	0	0	0	75.29	44.69	49.69
21	18	0	0	-2	0	54.09	39.09	42.49
10	19	1	-1	-1	1	43.97	51.97	74.47
6	20	1	-1	1	-1	48.81	32.33	60.43
3	21	-1	1	-1	-1	62.97	32.97	32.87
14	22	1	-1	1	1	54.57	62.17	90.27
19	23	0	-2	0	0	46.69	41.69	77.29
26	24	0	0	0	0	75.26	69.07	92.63
1	25	-1	-1	-1	-1	46.57	43.05	55.55
5	26	-1	-1	1	-1	71.25	31.17	57.27
12	27	1	1	-1	1	77.65	55.17	57.07
2	28	1	-1	-1	-1	24.13	44.21	58.71
30	29	0	0	0	0	77.71	68.15	90.76
18	30	2	0	0	0	47.69	60.29	73.29

Table 2. Analysis of variance for the optimization of MET degradation

Source	df	PTA		Cr_2O_3 NPs		PTA/ Cr_2O_3 NPs	
		p-value	Significant	p-value	Significant	p-value	Significant
Model	14	< 0.0001	+	< 0.0001	+	< 0.0001	+
A	1	< 0.0001	+	< 0.0001	+	< 0.0001	+
B	1	< 0.0001	+	< 0.0001	+	< 0.0001	+
C	1	< 0.0001	+	< 0.0001	+	< 0.0001	+
D	1	< 0.0001	+	< 0.0001	+	< 0.0001	+
AB	1	< 0.0001	+	0.0052	+	< 0.0001	+
AC	1	0.0338	+	0.1793	-	0.3478	-
AD	1	0.5864	-	0.1793	-	0.0716	-
BC	1	< 0.0001	+	< 0.0001	+	< 0.0001	+
BD	1	0.4485	-	0.1793	-	0.0716	-
CD	1	< 0.0001	+	< 0.0001	+	< 0.0001	+
A^2	1	< 0.0001	+	< 0.0001	+	< 0.0001	+
B^2	1	< 0.0001	+	< 0.0001	+	< 0.0001	+
C^2	1	< 0.0001	+	< 0.0001	+	< 0.0001	+
D^2	1	< 0.0001	+	< 0.0001	+	< 0.0001	+
Residual	15						
Lack of Fit	10	0.8469	-	0.0793	-	0.3878	-
Pure Error	5						
Cor Total	29						

PE% (Cr_2O_3 nanoparticles) = 69.3383 + 3.23333 * A + 4.73333 * B + 6.03333 * C + 8.73333 * D + 2.32 * AB - 1 * AC - 1 * AD + 6.12 * BC - 1 * BD + 4.52 * CD - 4.37875 * A^2 - 4.37875 * B^2 - 4.37875 * C^2 - 4.37875 * D^2 (3)

PE% (PTA/ Cr_2O_3 nanoparticles) = 90.2283 + 5.23333 * A - 7.23333 * B + 9.16667 * C + 10.5667 * D + 3.32 * AB + 0.5 * AC + 1 * AD + 4.62 * BC - 1 * BD + 4.02 * CD - 7.10125 * A^2 - 7.10125 * B^2 - 7.10125 * C^2 - 6.60125 * D^2 (4)

The coefficient of determination (R^2) and adjusted determination coefficient (adjusted R^2) were used to evaluate the fitted model with PE% as outcomes. The obtained R^2 and adjusted R^2 for all equations were equal to or higher than 0.9830 and 0.9620, respectively, indicating the models are fitted well with the responses (Table 3).

Also, the predicted determination coefficients (predicted R^2) were equal to or higher than 0.8967, showing the equations predict the future outcomes (PE%) well.

Table 3. Determination coefficients of the models for the optimization of MET degradation

Catalyst	Std. Dev.	Mean	C.V. %	R^2	Adjusted R^2	Predicted R^2	Adeq Precision
PTA	2.25	64.71	3.47	0.9850	0.9710	0.9466	31.6416
Cr_2O_3 NPs	2.84	55.33	5.13	0.9803	0.9620	0.8967	26.2371
PTA/Cr_2O_3 NPs	2.06	67.90	3.04	0.9943	0.9890	0.9739	44.1336

Table 4. Optimum values of each factor for the MET degradation

Factor	Name	TPA		Cr_2O_3 NPs		TPA/Cr_2O_3 NPs	
		Level	value	Level	Value	Level	Value
A	MET concentration (mg L^{-1})	-0.0460	195	0.0480	205	-0.4182	159
B	pH	0.4651	6.7	0.3258	6.3	-0.8069	3.5
C	H_2O_2 concnetration (mol L^{-1})	-0.2276	0.38	0.7230	0.47	0.1906	0.42
D	Catalyst amount (mg)	0.5401	177	0.7526	188	0.7269	186

According to Eq. (2), the critical interaction for the MET degradation is the interaction between pH and H_2O_2 concentration (BC) due to the highest coefficient in all equations. The interaction has a positive effect on the MET degradation using Cr_2O_3 nanoparticles or PTA/Cr_2O_3 nanoparticles and a negative effect in the presence of PTA (Figure 5). According to Figure 5 a, as the pH increases and the H_2O_2 concentration decreases simultaneously, the MET degradation efficiency using PTA increases. In concert, the degradation efficiency of MET using PTA/Cr_2O_3 nanoparticles was increased by a reduction in pH and an increase in the H_2O_2 concentration (Figure 5c). Finally, the degradation efficiency of MET using Cr_2O_3 nanoparticles increases with the simultaneous increase of both factors (Figure 5b) based on the obtained results and equations, the optimum values of factors to degrade MET using each catalyst were determined and presented in Table 4.

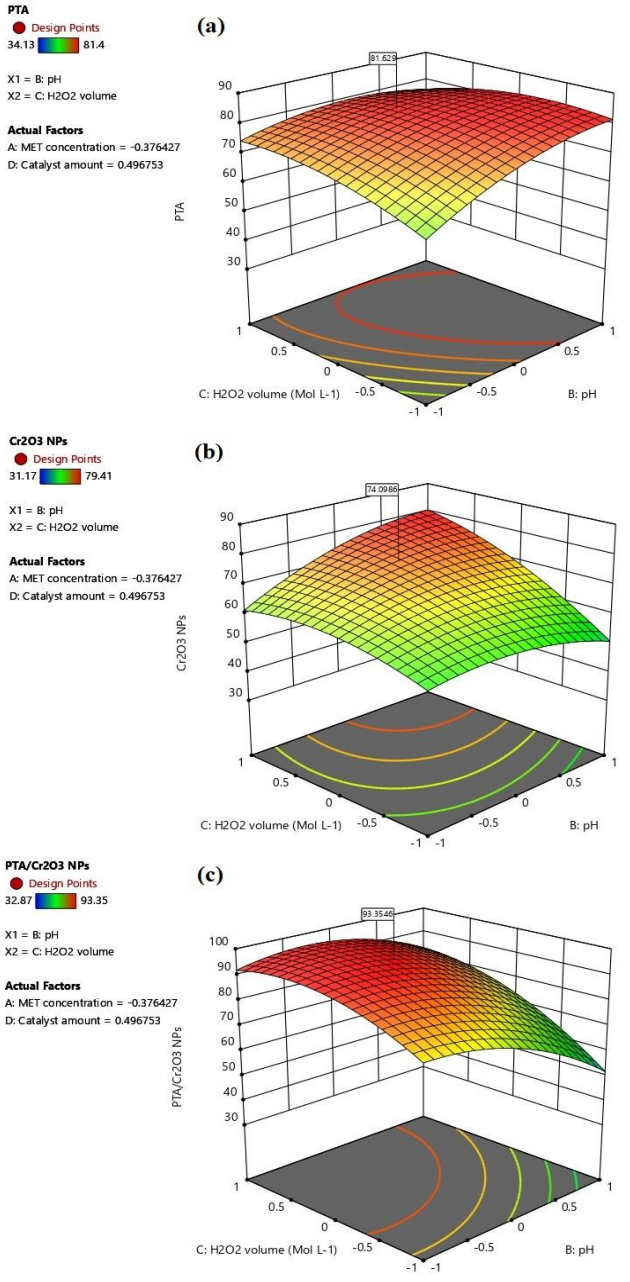

Figure 5. Interaction between pH and H_2O_2 in the presence of PTA (a), Cr_2O_3NPs (b), and PTA/Cr_2O_3NPs (c).

Kinetic of photocatalytic degradation

The degradation procedure is a time-dependent process. Therefore, the MET degradation was investigated in the time range 0-120 min using PTA, Cr_2O_3 nanoparticles, or PTA/Cr_2O_3 nanoparticles as a photocatalyst under optimum conditions. For this purpose, the Langmuir-Hinshelwood model is chosen to evaluate the kinetic behavior of the MET degradation in water samples using the prepared catalysts. According to the model, the change in MET concentration in water samples over degradation time in the presence of heterogeneous catalysts is determined to calculate the pseudo-first-order rate constant using the following equation:[32]

$$-\ln\left(\frac{C}{C_0}\right) = kt \qquad (5)$$

In the equation, C_o, C, and K are the MET initial concentration (t = 0) and the MET concentration at time (t > 0), and pseudo-first-order rate constant, respectively. The investigations were performed under the optimum conditions obtained for each catalyst (Table 4). Each experiment was carried out three times, and the average of the results was used to plot changes of - $\ln(C/C_o)$ versus degradation time. Also, EP% was calculated to compare the catalytic activity of the prepared photocatalysts for the

MET degradation using Eq. (1). The MET concentration was determined by UV-Vis spectrophotometry with an interval of 10 min from the beginning of exposure using a UVC lamp under stirring with 200 rpm. The sampling was performed using a pipette with a volume of 2 mL each 10 min with stopping the stirrer. The solution was transferred into a conical tube and centrifuged at 5000 rpm for 6 min to separate the catalyst before determining at 292 nm in 0.1 M HCl by a UV-Vis spectrophotometer. The results of the kinetic study for the MET degradation using PTA, Cr_2O_3 nanoparticles, or PTA/Cr_2O_3 nanoparticles as a photocatalyst are shown in Figure 6, indicating that the highest degradation rate is obtained in the presence of PTA/Cr_2O_3 nanoparticles. The results (Table 5) showed that the maximum EPs% for the MET degradation using PTA and Cr_2O_3 nanoparticles at a degradation time of 120 min were 82.00 and 77.18%, respectively. In concert, the maximum EP% of 90.11% for the MET degradation in the presence of PTA/Cr_2O_3 nanoparticles as a photocatalyst was obtained for 100 min, indicating the new hybrid material prepared from combining PTA and Cr_2O_3 nanoparticles, leading to a proper increase in the MET degradation and reducing the degradation time significantly. The highest pseudo-first-order rate constant was determined for the MET degradation using PTA/Cr_2O_3 nanoparticles as a photocatalyst. Besides, the lowest pseudo-first-order rate constant and EP% was obtained for Cr_2O_3 nanoparticles for the MET degradation. Obviously, tungsten(VI) in PTA has a full oxidization configuration (d°), leading to a convenient position for intramolecular charge transfer between unbonded electron pairs of oxygen atoms in ligands (HOMO orbital of O^{2-}) with empty orbitals in tungsten (LUMO orbital of W^{6+}).[33]

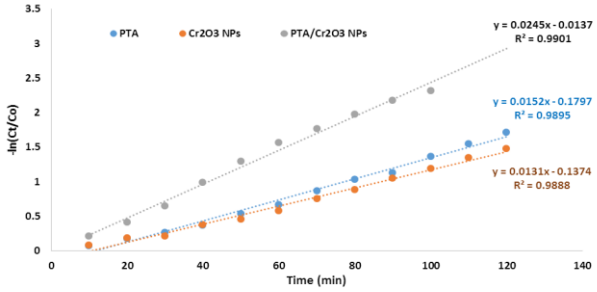

Figure 6. The MET degradation kinetics using PTA, Cr_2O_3NPs, and PTA/Cr_2O_3NPs.

Also, an improvement in the degradation rate and EP% of MET degradation in the presence of PTA/Cr_2O_3 nanoparticles may be due to the effect of Cr_2O_3 nanoparticles as a suitable host on the catalyst structure and encapsulation of PTA.[34]

The catalyst reusability

The reusability of the catalyst is a crucial parameter in the degradation application to degrade pollution in water samples. The catalyst was used to degrade MET according to section 2.3. The catalyst was then separated from the solution using centrifuging for 8 min at 6000 rpm, washed with methanol and distilled water, respectively, and dried at 80 °C before reuse. The maximum EP% of MET using PTA/Cr_2O_3 nanoparticles as a photocatalyst for five cycles was 90.11, 88.42, 84.06, 79.51, and 65.34%, respectively. The results indicated that PTA/Cr_2O_3 nanoparticles as a photocatalyst could apply for the MET degradation for four cycles without significantly reducing the degradation efficiencies.

The catalyst comparison with other catalysts

Very few studies have been performed on MET photodegradation. We were able to find only two studies for MET degradation under radiation. The first study was done in the absence of a photocatalyst. The results are shown in Table 6, showing that the use of catalysts can have a meaningful effect on the degradation time and degradation efficiency of MET. However, the catalysts used in this study significantly reduced the degradation time.

4. CONCLUSIONS

In the study, three catalysts, including PTA, Cr_2O_3nanoparticles, or PTA/Cr_2O_3 nanoparticles, were prepared to degrade MET in water samples. For this purpose, a simple hydrothermal procedure was used to synthesize these catalysts. Effective factors on the MET degradation were optimized using an experimental design

Table 5. The kinetic results of the MET degradation

Catalyst	Degradation time (min)	TRA dagradation (%)	Equation	R^2	K (min^{-1})
TPA	120	82.00	Y = 0.0152x-0.1797	0.9895	0.0152
Cr_2O_3 nanoparticles	120	77.18	Y = 0.0131x-0.1374	0.9888	0.0131
TPA/Cr_2O_3 nanoparticles	100	90.11	Y = 0.0245x-0.0137	0.9901	0.0245

Table 6. Comparison of the method with other methods

Catalyst	Radiation	pH	Catalyst amount (mg)	Degradation time (min)	Degradation efficiency (%)	Ref.
-	UVB	-	-	32 h	70	35
Free chlorine	Sunlight	4	5 µM	3 h	99	36
-	Sunlight	4	-	5 h	-	
TPA	UVC	6.7	177	120	82.00	This work
Cr_2O_3 nanoparticles	UVC	6.3	188	120	77.18	
TPA/Cr_2O_3 nanoparticles	UVC	3.5	186	100	90.11	

strategy based on a central composite design for three catalysts. The design included 30 runs that were performed in random order to remove the effects of uncontrollable parameters. Under the optimum conditions, the kinetic and EP% were investigated for the MET degradation using three catalysts, indicating that PTA/Cr_2O_3 nanoparticles has the highest EP% and rate constant compared to PTA or Cr_2O_3 nanoparticles as a catalyst. EP% of the MET degradation and the pseudo-first-order rate constant in the presence of PTA/Cr_2O_3 nanoparticles as a photocatalyst was equal to 90.11% for 100 min and 0.0245 cm^{-1}, respectively.

CONFLICTS OF INTEREST

There is no conflict of interest to declare.

ACKNOWLEDGMENTS

The Azad University of Mashhad, Iran, is appreciated for its support.

AUTHOR INFORMATION

Corresponding Author

Hassan Ali Zamani: Email: haszamani93@gmail.com, *ORCID*: 0000-0002-3156-2781

Author(s): Farshid Kazemi, Mohammad Reza Abedi, Mahmoud Ebrahimi

REFERENCES

1. J. Ferreira, *Pain Physician*, **2017**, *20*, 207-215.
2. C. Leventelis, N. Goutzourelas, A. Kortsinidou, Y. Spanidis, G. Toulia, A. Kampitsi, C. Tsitsimpikou, D. Stagos, A. S. Veskoukis, D. Kouretas,*Oxid. Med. Cell. Longev*.**2019**, Article ID 9417048.
3. I. Kamika, S. Azizi, A. A. Muleja, R. Selvarajan, M. A. El-Liethy, B. B. Mamba, T. T. Nkambule, *Environ. Pollut.*, **2021**, *290*, 118048.
4. K. Kaur, R. Badru, P. P. Singh, S. Kaushal, J. *Environ. Chem. Eng.*, **2020**, *8*, 103666.
5. G. Zhang, X. Zhang, Y. Meng, G. Pan, Z. Ni and S. Xia, *Chem. Eng. J.*, **2020**, *392*, 123684.
6. R. Abazari, S. Sanati, L. A. Saghatforoush, *Chem. Eng. J.*, **2014**, *236*, 82-90.
7. E. Safaralizadeh, S. J. Darzi, A. R. Mahjoub, R. Abazari, *Res. Chem. Interm.*, **2017**, *43*, 1197-1209.
8. P. Singh, A. Borthakur, *J. Clean. Prod.*, **2018**, *196*, 1669-1680.
9. P. Mahbub, P. Nesterenko, *RSC Adv.*, **2016**, *6*, 77603-77621.
10. R. Abazari, S. Sanati, A. Morsali, A. M. Kirillov, *Inorg. Chem.*, **2021**, *60*, 2056-2067.
11. R. Abazari, A. R. Mahjoub, S. Sanati, *Rsc Adv.*, **2014**, *4*, 56406-56414.
12. K. K. Kefeni, B. B. Mamba, *Sustain. Mater. Technol.*, **2020**, *23*, e00140.
13. G. Sharma, A. Kumar, S. Sharma, M. Naushad, R. P. Dwivedi, Z. A. ALOthman, G. T. Mola, *J. King Saud Univ. Sci.*, **2019**, *31*, 257-269.
14. E. Hosseini, M. Chamsaz, M. Ghorbani, *Eurasian J. Anal. Chem.*, **2017**, *13*, 1-10.
15. N. Rajput, *Int. J. Adv. Eng. Technol.*, **2015**, *7*, 1806.
16. J. Liu, J. Jiang, Y. Meng, A. Aihemaiti, Y. Xu, H. Xiang, Y. Gao, X. Chen, *J. Hazard. Mat.*, **2020**, *388*, 122026.
17. M. Ghorbani, A. Shams, O. Seyedin, N. Afshar Lahoori, *Environ. Sci. Pollut. Res.*, **2017**, *25*, 5655.
18. S. Rajagopal, M. Bharaneswari, D. Nataraj, O. Khyzhun, Y. Djaoued, *Mat. Res. Exp.*, **2016**, *3*, 095019.
19. H. N. Deepak, K. Choudhari, S. Shivashankar, C. Santhosh, S. D. Kulkarni, *J. Alloys Comp.*, **2019**, *785*, 747-753.
20. A. S. Gomes, N. Yaghini, A. Martinelli, E. Ahlberg, *J. Raman Spect.*, **2017**, *48*, 1256-1263.
21. A. Helal, F. A. Harraz, A. A. Ismail, J. *Photochem. Photobiol. A*, **2021**, *419*, 113468.
22. J. Lan, Y. Wang, B. Huang, Z. Xiao, P. Wu, *Nanoscale Adv.*, **2021**, *3*, 4646-4658.
23. B. Huang, D. -H. Yang, B. -H. Han, *J. Mat. Chem. A*, **2020**, *8*, 4593-4628.
24. A. -E. Stamate, O. D. Pavel, R. Zavoianu, I. -C. Marcu, *Catalysts*, **2020**, *10*, 57.
25. L. Zhai, H. Li, Molecules, **2019**, *24*, 3425.
26. J. -J. J. Chen, M. A. Barteau, J. Energy Storage, **2017**, *13*, 255-261.
27. N. Lotfian, M. M. Heravi, M. Mirzaei, B. Heidari, *Appl. Organomet. Chem.*, **2019**, *33*, e4808.
28. A. Ayati, B. Tanhaei, F. F. Bamoharram, A. Ahmadpour, P. Maydannik, M. Sillanpää, *Sep. Purif. Technol.*, **2016**, *171*, 62-68.
29. Y. Orooji, B. Tanhaei, A. Ayati, S. H. Tabrizi, M. Alizadeh, F. F. Bamoharram, F. Karimi, S. Salmanpour, J. Rouhi, S. Afshar, *Chemosphere*, **2021**, *281*, 130795.
30. F. A. Alharthi, H. S. Alanazi, A. A. Alsyahi, N. Ahmad, *Crystals*, **2021**, *11*, 456.
31. Z. Pei, H. Xu, Y. Zhang, *J. Alloys Comp.*, **2009**, *468*, L5-L8.
32. R. S. Khoshnood, D. S. Khoshnoud, *Appl. Phys. A*, **2019**, *125*, 750.
33. K. Suzuki, N. Mizuno, K. Yamaguchi, *ACS Catal.*, **2018**, *8*, 10809-10825.
34. Z. -J. Lin, H. -Q. Zheng, J. Chen, W. -E. Zhuang, Y. -X. Lin, J. -W. Su, Y. -B. Huang, R. Cao, *Inorg. Chem.*, **2018**, *57*, 13009-13019.
35. D. Favretto, M. Tucci, A. Monaldi, S. D. Ferrara, G. Miolo, *Drug Test. Anal.*, **2014**, *6*, 78-84.
36. M. -C. Hsieh, S. C. Panchangam, W. W. -P. Lai, A. Y. -C. Lin, *Chemosphere*, **2018**, *209*, 104-112.